

Setup of a new Brillouin light scattering apparatus with submicrometric lateral resolution and its application to the study of spin modes in nanomagnets

Gianluca Gubbiotti, Giovanni Carlotti, Marco Madami, Silvia Tacchi, Paolo Vavassori et al.

Citation: *J. Appl. Phys.* **105**, 07D521 (2009); doi: 10.1063/1.3068428

View online: <http://dx.doi.org/10.1063/1.3068428>

View Table of Contents: <http://jap.aip.org/resource/1/JAPIAU/v105/i7>

Published by the [American Institute of Physics](#).

Additional information on J. Appl. Phys.

Journal Homepage: <http://jap.aip.org/>

Journal Information: http://jap.aip.org/about/about_the_journal

Top downloads: http://jap.aip.org/features/most_downloaded

Information for Authors: <http://jap.aip.org/authors>

ADVERTISEMENT



AIP Advances

Now Indexed in Thomson Reuters Databases

Explore AIP's open access journal:

- Rapid publication
- Article-level metrics
- Post-publication rating and commenting

Setup of a new Brillouin light scattering apparatus with submicrometric lateral resolution and its application to the study of spin modes in nanomagnets

Gianluca Gubbiotti,¹ Giovanni Carlotti,^{1,a)} Marco Madami,¹ Silvia Tacchi,¹ Paolo Vavassori,^{2,3} and Giovanni Socino¹

¹*Dipartimento di Fisica, CNISM, Università di Perugia, I-06123 Perugia, Italy*

²*Research Center S3-INFM-CNR, I-41100 Modena, Italy*

³*Dipartimento di Fisica, Università di Ferrara, I-44100, Italy and CIC nanoGUNE Consolider, San Sebastian, E-20009, Spain*

(Presented 11 November 2008; received 17 September 2008; accepted 5 November 2008; published online 24 February 2009)

A new microfocused Brillouin light scattering (BLS) apparatus has been setup using a microscope objective with large numerical aperture and achieving a submicrometric lateral resolution, as inferred by reflectivity measurements taken on a set of calibration arrays consisting of Al stripes with different spacings. The micro-BLS apparatus has been then used to investigate the magnetic normal modes of elliptical Permalloy nanorings. The superiority of micro-BLS over conventional BLS measurements in the detection of stationary modes, especially those localized close to the edges of the nanoring where the internal field is highly nonhomogeneous, is demonstrated. A satisfactory interpretation of the measured spectra in terms of dynamical magnetization distribution inside the rings was achieved by a comparison with the output of dynamical micromagnetic simulations. © 2009 American Institute of Physics. [DOI: [10.1063/1.3068428](https://doi.org/10.1063/1.3068428)]

I. INTRODUCTION

The Brillouin light scattering (BLS) technique is one of the most powerful tools used nowadays to investigate the high-frequency dynamical properties of artificially prepared magnetic nanostructures, such as dots, stripes, etc. It relies on the inelastic scattering of photons by thermal magnons (spin waves) naturally present within the medium under investigation. Unfortunately in conventional BLS measurements the lateral resolution is poor, the illuminated area of the sample being several tens of micrometers wide. Therefore, BLS experiments are usually performed on large arrays of (hopefully) identical elements and give access to average properties of the ensemble. The identification of the measured peaks in terms of specific eigenmodes of each dot is usually done in an indirect way: the measured frequencies are compared with those calculated by either analytical or numerical calculations and the corresponding mode profile is inferred from the latter. Demidov *et al.*¹ at Kaiserslautern University first demonstrated the possibility of achieving submicrometric resolution in BLS measurements, using a focusing objective with a large numerical aperture. This opened the way to new kinds of investigations aimed to directly visualize the spatial profile of the dynamical magnetization of stationary eigenmodes in laterally confined structures, such as squares² and circular rings.³

Here we report about the setup of a novel micro-BLS apparatus with a submicrometric lateral resolution at Ghost Laboratory of Perugia University. The main features of this new apparatus are discussed, showing that most of the col-

lected signal comes from a sample region less than 250 nm wide. Preliminary results relative to the study of stationary eigenmodes in elliptical Permalloy (NiFe) nanorings are compared with those of conventional BLS measurements. Emphasis is given to the possibility of directly visualizing the spatial extent of the different modes inside the nanomagnet, including the higher sensitivity of our micro-BLS apparatus for the detection of localized modes, as well as to the good agreement between measurements and micromagnetic simulations.

II. EXPERIMENTAL DETAILS

BLS measurements were performed in the backscattering configuration using a (3+3)-pass Sandercock type Fabry-Pérot interferometer. A collimated beam of monochromatic light from a diode-pumped solid-state laser (wavelength of 532 nm, power of 150 mW) was focused on the sample surface and an external magnetic field \mathbf{H} was applied parallel to the sample plane and normal to the incidence plane of light. For conventional measurements, we used a camera objective with f -number 2 and 50 mm focal distance, which leads to an illuminated area of about $30 \times 30 \mu\text{m}^2$ and a light incidence angle of $\theta=40^\circ$. For the micro-BLS measurements, instead, a Mitutoyo 100 \times objective, with numerical aperture NA=0.70 and super-long working distance (6 mm) was used, focusing about 5 mW of light perpendicularly on the sample surface. Using the same objective, we also built a coaxial viewing system based on a white light source, a 20 \times beam expander and a charge coupled device (CCD) camera, to obtain a direct visualization of the sample region under investigation. The system allows the direct observation of the surface of the sample (field of view of about 10

^{a)}Author to whom correspondence should be addressed. Electronic mail: carlotti@fisica.unipg.it. Tel./FAX: +39 075 585 2767.

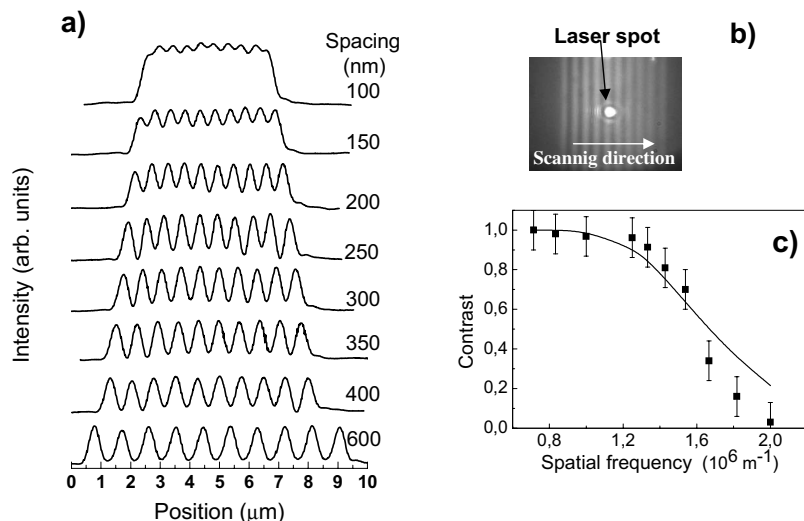


FIG. 1. (a) Sequence of reflectivity curves for different stripes array as a function of the edge-to-edge spacing between the stripes. (b) Image recorded by the CCD camera for the stripes separated by 600 nm and (c) experimental (points) and calculated (curve) contrast plotted vs the spatial frequency of the stripes array.

$\times 10 \mu\text{m}^2$) and the position of the probing laser spot on the screen of a monitor during measurements [see Fig. 1(b)].

III. RESULTS AND DISCUSSION

To obtain quantitative information about the lateral sensitivity achievable with the new apparatus, we used a set of calibration gratings prepared using e-beam lithography by Gubbiotti *et al.*⁵ at the Department of Electrical and Computer Engineering of the Singapore University. Each grating consists of ten Al stripes, 400 nm wide and 40 nm thick, with variable separation s in the range between 100 nm and $1 \mu\text{m}$, deposited on a Si substrate. The intensity of the reflected light was measured by a photodiode while scanning the laser spot across the stripes. Due to the different reflection coefficients between Al and Si, a marked modulation in the reflected intensity was observed. First of all, we measured the shape profile of our focused laser beam by simply scanning the spot over the step between the Si substrate and one Al line. In such a way we could reconstruct the intensity profile of the Gaussian laser beam, whose full width at $1/e^2$ of its maximum intensity turned out to be $2w = 400 \pm 20$ nm, corresponding to a full width at half maximum (FWHM) of about 235 ± 12 nm. To further characterize the lateral sensitivity of this apparatus, we then recorded a sequence of reflectivity measurements while scanning the laser spot position across the different gratings, as reported in Figs. 1(a) and 1(b). It can be seen that the measured curves present oscillations whose amplitude tends to rapidly decrease when the separation between Al stripes becomes lower than 250 nm, i.e., lower than the FWHM of the illuminating light beam. More quantitatively, one can calculate the contrast C , which is defined as $C = (I_{\text{max}} - I_{\text{min}}) / (I_{\text{max}} + I_{\text{min}})$, where I_{max} and I_{min} are the normalized maximum and the minimum intensity, respectively, measured by the photodiode. For instance, it can be easily estimated that when the separation s would coincide exactly with the FWHM of the Gaussian focused beam (235 nm), about 75% of the total intensity falls in the gap between two Al stripes so that the expected contrast is $C = 0.6$. If one plots the contrast C versus the spatial frequency (reciprocal of the spatial period of the grating) one obtains the so-called contrast transfer function

(CTF). A direct comparison between the calculated CTF (Ref. 4) and the experimental values is shown in Fig. 1(c), exhibiting a fairly good agreement. An independent estimate of the lateral sensitivity of the micro-BLS apparatus was obtained from detection of spin waves in an array of adjacent Co and NiFe stripes, $2 \mu\text{m}$ wide (not shown here due to length limitation). We measured the spatial extent where the coexistence of the signal from the two different materials

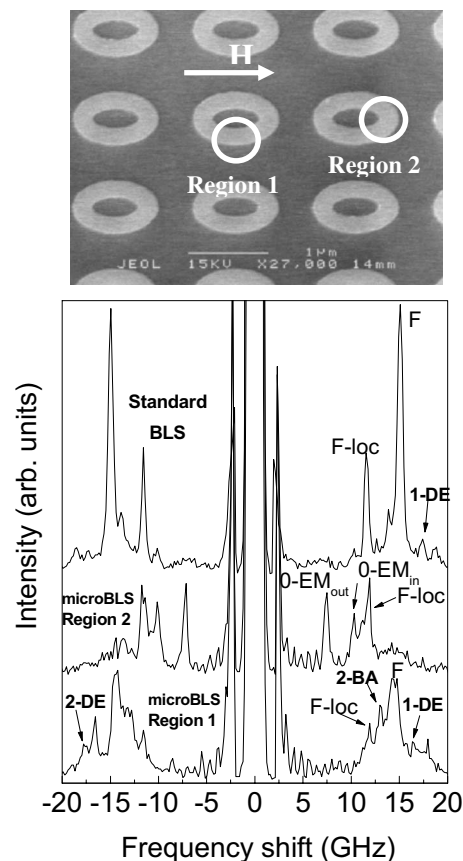


FIG. 2. Top panel: SEM of the elliptical permalloy rings. Two regions are highlighted, corresponding to those where the micro-BLS spectra were recorded in the presence of a magnetic field $H = 1.6$ kOe applied along the arrow direction. Bottom panel: comparison between the spectrum measured with the conventional BLS apparatus and two micro-BLS spectra measured at regions 1 and 2 of the ring.

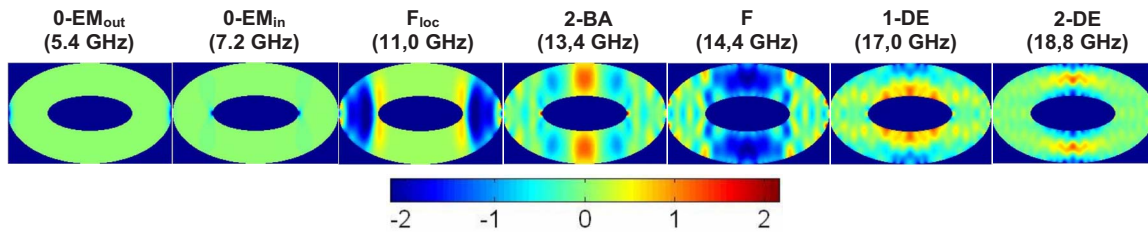


FIG. 3. (Color online) Calculated out-of-plane component of the dynamic magnetization of various spin modes for an external magnetic field $H=1.6$ kOe applied along the major axis of the ellipses. The mode labels and the corresponding frequency is indicated over each panel.

could be observed in the spectra while scanning the light spot across the boundary between adjacent stripes, at steps of 50 nm. Such an extent turned out to be about 250 nm, a value which roughly coincides with the FWHM of our Gaussian beam, where most of the light energy is indeed concentrated. Finally, to test the capability of our prototypical apparatus in the detection of laterally confined stationary magnetic modes, we analyzed an array of elliptical NiFe rings with outer (inner) axes of 1060×660 nm² (550×230 nm²). The rings, whose scanning electron microscope (SEM) image is shown in the top panel of Fig. 2, were fabricated by a combination of *e*-beam lithography, *e*-beam evaporation, and lift-off processes at the Institute for Chemical Research of the Kyoto University (Japan). An external magnetic field $H = 1.6$ kOe was applied along the major axis of the rings (as indicated in the top panel of Fig. 2) to obtain the “onion state,” i.e., an almost saturated state, characterized by a uniform magnetization distribution in the two rings arms parallel to the applied field (region 1) and two opposite head-on-head (180°) domain walls at the rings edges (region 2), where the internal field is drastically reduced as a consequence of demagnetizing effect. In the lower panel of Fig. 2, we present a comparison between the spectra measured by conventional-BLS (top spectrum) and those recorded by micro-BLS in regions 1 and 2. Remarkably, the spectra relative to these two regions (whose centers are less than 450 nm afar from each other) are very different, with some peaks appearing only in one of the two regions, confirming the high lateral resolution of our apparatus. To achieve a detailed understanding of these features, a dynamical micromagnetic simulation, which solves the discretized Landau–Lifshitz–Gilbert equation in the time domain and locally calculates the Fourier transform, was performed. The detailed procedure for this calculation is described in Ref. 5. Both the frequency and the spatial distribution of the different eigenmodes could be obtained (Fig. 3) and classified according to previous literature.^{6–9} In particular, one can first recognize some modes extending in region 1, where the internal field is almost uniform and parallel to the external field. These can be roughly classified as: backwardlike modes (*m*-BA) with *m* nodal lines perpendicular to H , Damon–Eshbach-like modes (*n*-DE) with *n* nodal lines parallel to the direction of H , and fundamental mode (F), without nodes, analogous to the Kittel uniform one. In addition, other modes exist in the shorter arms of the rings, i.e., in region 2, where the internal field is highly inhomogeneous. These are the so called localized fundamental mode (F -loc) and the end modes (EM) confined at

either the outer or the inner border of the ring. From a comparison with the simulation output, summarized in Fig. 3, it turns out that the spectrum recorded in region 1 is dominated by the F mode (at about 14.4 GHz) and exhibits also the peaks associated to two DE -like modes (16.6 and 18.0 GHz) and to a BA mode (13.15 GHz). It is interesting to remark that in this spectrum there are no peaks observed below 10 GHz. On the contrary, two intense low-frequency peaks due to both outer and inner 0- EM appear in the spectrum relative to region 2, i.e., close to the dot edges.¹⁰ Remarkably, the 0- EM modes are also missed in the standard BLS spectrum because their marked localization and dependence on the morphology of each individual dot correspond to a very feeble and broad peak in standard measurements, which are averaged over thousands of rings. This proves the supremacy of micro-BLS over standard BLS in the analysis of stationary modes in nanomagnets.

The authors gratefully acknowledge Professor O. Adeyeye and Professor T. Ono for sample preparation, as well as Italian Ministero dell’Istruzione, Università e Ricerca, and Consorzio Interuniversitario di Scienze Fisiche della Materia (CNISM) for financial support through Progetto Innesco.

¹V. E. Demidov, S. O. Demokritov, B. Hillebrands, M. Laufenberg, and P. Freitas, *Appl. Phys. Lett.* **85**, 2866 (2004).

²K. Perzlmaier, M. Buess, C. H. Back, V. E. Demidov, B. Hillebrands, and S. O. Demokritov, *Phys. Rev. Lett.* **94**, 057202 (2005).

³H. Schultheiss, S. Schafer, P. Candeloro, B. Leven, B. Hillebrands, and A. N. Slavin, *Phys. Rev. Lett.* **100**, 047204 (2008).

⁴The calculation of the CTF was performed by evaluating the convolution integral between the Gaussian profile representing our focused laser beam and the step function representing the grating. A detailed discussion concerning the connection between CTF and resolution in light microscopy experiments can be found in E. H. K. Stelzer, *J. Microsc.* **189**, 15 (1998).

⁵G. Gubbiotti, M. Madami, S. Tacchi, G. Carlotti, M. Pasquale, N. Singh, S. Goolaup, and A. O. Adeyeye, *J. Phys.: Condens. Matter* **19**, 406229 (2007).

⁶I. Neudecker, M. Klau, K. Perzlmaier, D. Backes, L. J. Heydenman, C. A. F. Vaz, J. A. C. Bland, U. Rudiger, and C. H. Back, *Phys. Rev. Lett.* **96**, 057207 (2006).

⁷F. Giesen, J. Podbielski, T. Korn, and D. Grundler, *J. Appl. Phys.* **97**, 10A712 (2005).

⁸F. Montoncello, L. Giovannini, F. Nizzoli, H. Tanigawa, T. Ono, G. Gubbiotti, M. Madami, S. Tacchi, and G. Carlotti, *Phys. Rev. B* **78**, 104421 (2008).

⁹F. Montoncello, L. Giovannini, F. Nizzoli, P. Vavassori, M. Grimsditch, T. Ono, G. Gubbiotti, S. Tacchi, and G. Carlotti, *Phys. Rev. B* **76**, 024426 (2007).

¹⁰Note that the calculated frequency of the EMs is overestimated in the calculation because the dot edge is discretized in the simulation so that it fails to mimic satisfactorily the actual rounded elliptical profile.